Modeling and Simulation of the Coal Flow Control System for the Longwall Scraper Conveyor

Olimpiu Stoicuţă[*], Teodor Pană[†]
[*]University of Petrosani / Departament of Control Engineering, Computers, Electrical Engineering and Power Engineering
[†]Technical University of Cluj – Napoca / Departament of Electrical Machines and Drives
[*] OlimpiuStoicuta@upet.ro, [†] Teodor.Pana@edr.utcluj.ro

***Abstract* - In this paper, the modeling and simulation of a coal flow control system for the longwall scraper conveyor is presented. The coal flow on the scraper conveyor, it is controlled by the following variables: the coal flow, advance speed and cutting speed of the longwall shearer. The electrical drive system of the longwall scraper conveyor together with the electrical drive system of the advancement and the cutting mechanism of the longwall shearer are done by means of induction motors. The control of speeds and electromagnetic torque of induction motors is realized by using sensorless vector control systems. Within these control systems, the estimation of position and of components of the rotor flux space-phasor, as well as the rotor speed of the induction motor, is done by an extended Gopinath observer. The advantages of a coal flow control system are control of productivity and also that electric motors of the flow of transport can be optimally chosen, leading ultimately to a much lower consumption of electricity for coal extraction. Modeling and simulation of control systems is done taking into account the mathematical equations that make the connection between constructive and functional parameters of the longwall shearers with the features of the strata of mining coal, specifically the coal deposits from the Jiu Valley, Romania.**

Keywords: *coal flow control system; induction motor; sensorless vector control; longwall mining; longwall sharer; scraper conveyor*.

I. INTRODUCTION

A longwall mining system consists of the longwall shearers, scraper conveyor, powered roof supports and auxiliary equipment (see Fig.1) [1].

The current technology of extracting the coal in the longwall mining is based on three main technological processes that are made with the elements of a longwall system.

The three technological processes are [1]:

- extracting and loading coal onto a conveyor (of the longwall shearers);
- the coal transport (scraper conveyor);
- the roof support longwall mining (powered roof supports).

The longwall shearers are mining machines that are designed to dislodge, break and load the broken material on the means of transport.

The automation of the longwall shearers for the cutting of the coal layers from the longwall face is done in order to achieve the following objectives: achieving maximum productivity; getting minimum energy consumption; protection of electric motors and removing the human operator.

Fig. 1. The elements composing the longwall mining system [2].

Until now, the vast majority of firms producing the longwall shearers have partially solved the objectives mentioned above.

The constant control of the flow of coal on the scraper conveyor currently accounts for one of the most important issues in the field of automation of longwall systems.

The main objective of the article is presentation and analysis of a new control system for the flow of coal on the scraper conveyor of the longwall system. Automatic control of the flow of coal on the scraper conveyor is made by means of a control system where in the main loop there is a flow of coal, while the secondary loop is for advancement and cutting speed of the longwall shearers. The advancement and the cutting speed are considered components of the input vector of the longwall shearers, regarded by the control theory as an element execution. The control systems of induction motors speeds in the conveyor system, advancement system and the cutting system are built based on a sensorless vector control systems with direct rotor flux orientation.

Position estimation and dq components of rotor flux space-phasor, as well as the rotor speed of the induction motor are built on an extended Gopinath observer (EGO).

The constant control of the flow of coal on the scraper conveyor offers the optimal choice for the induction motors and of the gear reducers from the conveyor system of coal.

Analysis of the new control system is done by simulation on Matlab-Simulink. Modeling and simulation of control systems is done taking into account the mathematical equations that make the connection between constructive and functional parameters of the longwall shearers, with the features of the strata of coal, specifically the coal deposits of the Jiu Valley. The coal basin of Jiu Valley is located in Romania, in the southern part of Hunedoara County, in the South-West of Transylvania.

II. The Analysis Of The Cutting System

The cutting organs execute a movement of rotation around their own axis and a movement of advancement, due to the displacement of the longwall shearer.

The trajectory of a certain knife of the cutting organs (see Fig.2), performs a move of roto-translation defined by the following relations

$$\begin{cases} x(t) = v_a \cdot t + R_a \cdot \sin(\varphi) \\ y(t) = R_a \cdot \cos(\varphi) \end{cases} \quad (1)$$

Based on relations (1) we can write the following equation

$$\left(x(t) - v_a \cdot t\right)^2 + y^2(t) = R_a^2 \quad (2)$$

where $R_a = D/2$, and D is the diameter of the cutting organs measured from the tip of the splintering knife.

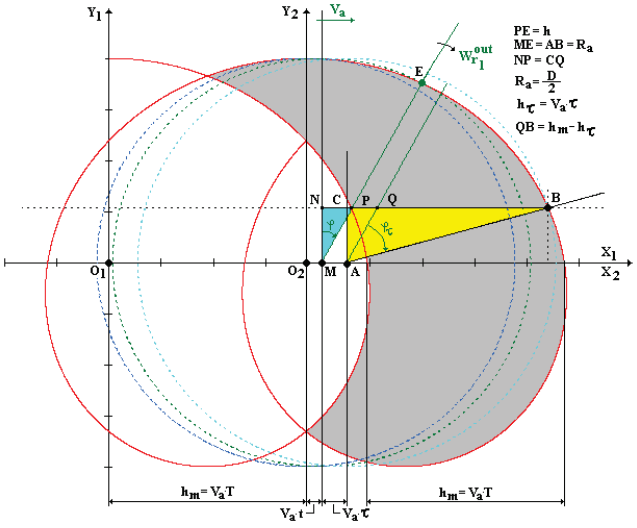

Fig.2. The analysis of the cutting system.

The relations (1), represent the coordinates of the point P in $X_2O_2Y_2$ axis system and the expression (2) is the equation of a circle with the variable center. Under these circumstances, the expression which define the splinter thickness cut in longitudinal section is [1]:

$$h = R_a + \left(h_m - h_\tau\right) \cdot \sin(\varphi) - \sqrt{R_a^2 - \left(h_m - h_\tau\right)^2 \cdot \cos^2(\varphi)} \quad (3)$$

where

$$h_m = v_a \cdot T \,;\, h_\tau = v_a \cdot \tau \,;\, T = \frac{2 \cdot \pi}{\omega_{r1}^{out}} \,;\, \omega_{r1}^{out} = \frac{d\varphi}{dt} \,;\, v_t = R_a \cdot \omega_{r1}^{out}.$$

Because at the longwall shearer the cutting speed is much greater than the advancement speed, the splinter thickness cut can be approximated by a sinusoidal function of the form:

$$h = h_m \cdot \sin(\varphi) \quad (4)$$

where $h_m = 2 \cdot \pi \cdot R_a \cdot \frac{v_a}{v_t}$

Where we also take into account the number of knives on the cutting line, the maximum splinter thickness cut is

$$h_m = k_b \cdot \frac{v_a}{v_t} \quad (5)$$

where $k_b = \frac{2 \cdot \pi \cdot R_a}{c}$, and c represents the number of knives on the cutting line.

From relation (5) it is observed that the ratio of the advancement speed and cutting speed can control the maximum splinter thickness cut by a longwall shearer.

From the practical researches of Kovacs and et. al.[1], the maximum value of the splinter thickness cut, for what we get minimum specific energy consumption at the splinter cutting, is

$$h_m = \frac{2 \cdot d - b}{\tan(\psi)} \quad (6)$$

for parallelepiped knives.

In relations (6) we used the following notations: d is the distance between the cutting lines, ψ is rake angle of the splinter in the transversal section, and b is the width of the cutting edge of the parallelepiped knife.

The practical researches of Kovacs and et. al. [1], shows that the slope of the talus angle of the splinter cut (for a cutting depth greater than 2 cm, see Fig.3), for the Jiu Valley coals, is $\tan(\psi) = 1.28$.

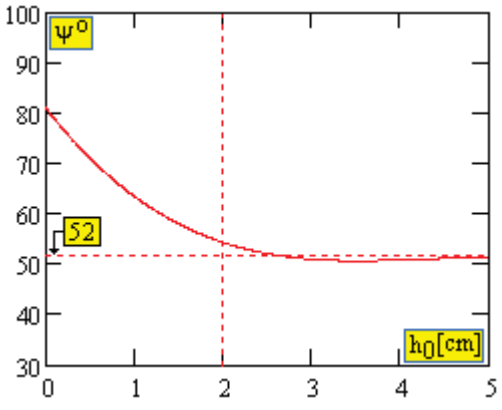

Fig.3. The variation of the talus angle depending of the cutting depth.

The relations (5) and (6) allow for prescribing the block of cutting speed according to the advancement speed.

The relation underlying implementation of the prescribing block (EP_a), in the case of parallelepiped knives, is:

$$v_t^* = \frac{k_b \cdot \tan(\psi)}{2 \cdot d - b} \cdot v_a^* \quad (7)$$

The block diagram of the control system for the cutting speed, respectively of the advance speed, are shown in Fig.4.

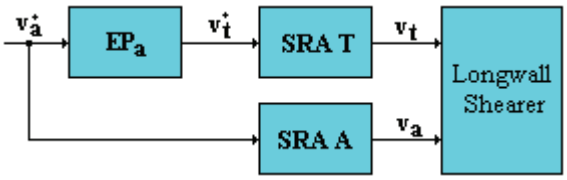

Fig.4. The block diagram of the optimal of the speed control system.

The control system shown in Fig.4, allows for the control of the maximum splinter thickness cut by controlling the advancement speed as well as the cutting speed [3]. In Fig. 4, by the "*SRA T*" and "*SRA A*" is noted cutting speed control system, respectively, advance speed control system.

III. The Cutting Speed Control System

This system is intended for dislocation of coal from the massive and for the coal loading onto the conveyor.

The drive of the cutting organs is usually done with the help of squirrel cage induction motors (M_1 and M_2), located inside cutting arms.

The electromagnetic torques developed by electric motors are submitted to the cutting organs (1 and 2), through some planetary transmissions and the coupling elements located inside the arms. The cutting control system of longwall shearers is presented in Fig 5.

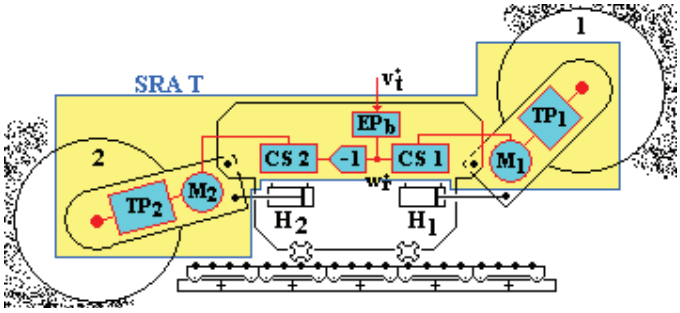

Fig.5. The block diagram of the cutting speed control system (SRA T).

The cutting organs are in form of a helicoidal rotor, and the cutting knives are arranged in a helicoidal shape.

The planetary transmissions TP_1 and TP_2 are considered identical, having an equal transmission report (see Fig.6).

In this paper, TP1 and TP2 the planetary transmissions are considered identical to the planetary transmissions of the longwall shearer KSW-460NE (see Fig.6). The control of speeds and electromagnetic torque of induction motors (M_1 and M_2) is realized using a sensorless vector control systems (CS_1 and CS_2). On the other hand, to be able to control the same speed for both cutting organs, the prescribing element of the two tuning systems (CS_1 and CS_2), has to be the same.

The prescribing element (EP_b) is defined by the following relation:

$$\omega_r^* = \frac{i_T}{R_a} \cdot v_T^* \quad (8)$$

where $R_a = D/2$, D is the diameter of the cutting organs measured from the tip of the splintering knife and i_T is the gear ratio for TP_1 and TP_2.

The gear ratio of the TP_1 and TP_2, prezented in the Fig. 6, is calculated by the following formula:

$$i_T = \left(1 + \frac{z_3}{z_1}\right) \cdot \frac{z_5}{z_4} \cdot \frac{z_{10}}{z_6} \cdot \left(1 + \frac{z_{13}}{z_{11}}\right) \quad (9)$$

where: z_i is the number of teeth in the gears.

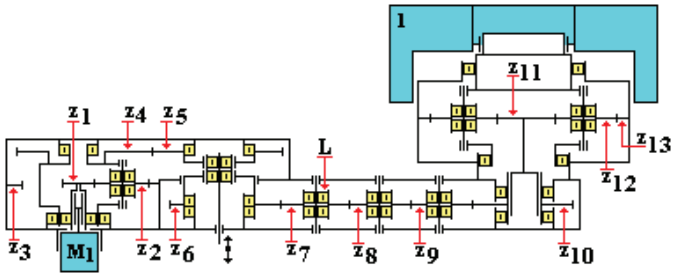

Fig.6. The block diagram of the planetary transmission TP_1 [4].

The equations that define the planetary transmissions (TP_1 and TP_2), are:

$$\omega_{r_k}^{out} = \frac{\omega_{r_k}^{in}}{i_T} \quad (10)$$

$$M_T^{out} = \eta_T \cdot i_T \cdot M_e \quad (11)$$

where: $k = \{1,2\}$; M_e is electromagnetic torque of the induction motor (M_1 or M_2); M_T^{out} is torque at the shaft of the cutting organs (1 and 2); η_T is the total efficiency of the planetary transmission (TP_1 or TP_2).

IV. The Advance Speed Control System

This system is intended for the displacement of the longwall shearers during work and mining of various maneuvers as well as for the maintenance of a permanent contact between the cutting body and massive. The displacement of the longwall shearers during operation can be done through some type of advancement systems, either mechanical, hydraulic or electric. If the case in which the coal layers have a small or medium tilt, the actuating system of the advance system component is mounted on the longwall shearers.

In recent years, the vast majority of the longwall shearers for the coal strata that have had a small or average inclination, having an advancement system that is electrically powered, generally a drive through two induction motors (M_L and M_R). The torque developed by the electric motor is transmitted to the advance mechanism mechanical with planetary equipment (TP_L and TP_R), see Fig.7. Between the advancement mechanisms, the most commonly used in European Union countries are: Rollrack mechanisms, Eicotrack and Dynatrack.

In this article, the drive system chosen for analysis is an electric one, developed around the two induction motors, and the advancement mechanism is of Eicotrack type.

The Eicotrack advance mechanism has been developed by the Eickhoff company and consists of two pinions - driving (R_L and R_R) that enter in gearing with a rack gear (3) fixed on the edge of the conveyor (rack and pinion mechanism). The pinions - driving are driven through planetary transmission and the two electric motors, see Fig.7. The raising and the lowering arms, on which are mounted cutting organs is usually done by means of hydraulic actuators (H_1 and H_2).

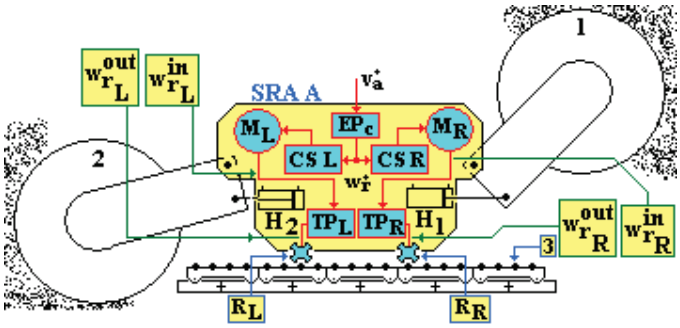

Fig.7. The block diagram of the advance speed control system (SRA A).

In the case of the advancement mechanisms, the rack pin has a circular profile and the tooth of the wheel has evolventic profiles, the line of gearing is determined by line (d), what is defined by the point of contact (P) and the axis pin (A), see Fig.8.

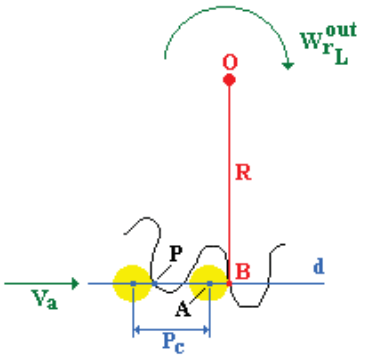

Fig.8. The interaction mode of the pinion with rack [3].

The rack with bolts that has the step (P_c) it is mounted into space exploited what improves the loading conditions of the coal on the conveyor while it eliminates the dangers of blocking. In the case of the advancement mechanism, the items located in the gear have the above mentioned profiles and advancement speed is given by the next relation

$$v_a = R \cdot \omega_{rL}^{out} \tag{12}$$

where ω_{rL}^{out} is the angular speed of the leader element, and R is the distance between points O and B what is constant during the whole phase of gearing.

The control of speeds and electromagnetic torque of induction motors (M_L and M_R) is realized using the sensorless vector control systems (CS_L and CS_R).

The prescribing element (EP_c) of the two control systems is the same and is defined by the following relation:

$$\omega_r^* = \frac{i_A}{R} \cdot v_a^* \tag{13}$$

where R is the distance between the points O and B, and i_A is the gear ratio for TP_L and TP_R.

In this paper, TP_L and TP_R, the planetary transmissions, are considered identical to the planetary transmissions of the longwall shearer KSW-460NE (see Fig.9).

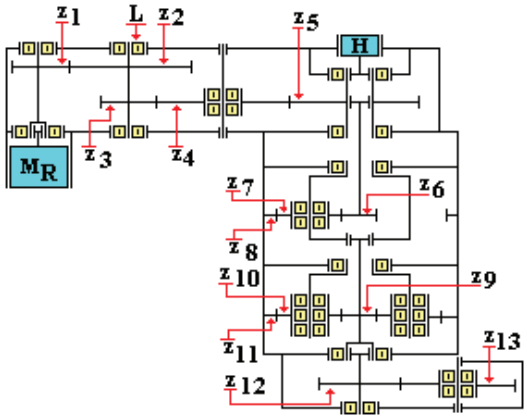

Fig.9. The block diagram of the planetary transmission TP_R [4].

The gear ratio of the TP_L and TP_R, prezented in the Fig. 9, is calculated by the following formula

$$i_A = \frac{z_2}{z_1} \cdot \frac{z_4}{z_3} \cdot \frac{z_5}{z_4} \left(1 + \frac{z_8}{z_6}\right) \cdot \left(1 + \frac{z_{11}}{z_9}\right) \cdot \frac{z_{13}}{z_{12}} \tag{14}$$

where: z_i is the number teeth of the gears.

The equations that define the planetary transmissions (TP_L and TP_R), are:

$$\omega_{r_k}^{out} = \frac{\omega_{r_k}^{in}}{i_A} \tag{15}$$

$$M_a^{out} = \eta_a \cdot i_A \cdot M_e \tag{16}$$

where: $k = \{L, R\}$; M_e is electromagnetic torque of the induction motor (M_L or M_R); M_a^{out} is torque at the shaft of the pinion (R_L or R_R); η_a is the total efficiency of the planetary transmission (TP_L or TP_R).

V. THE SENSORLESS VECTOR CONTROL SYSTEM

The automatic control of the advancement speed and of the cutting speed is done through the speeds control systems of the induction motors from the component of the advancement and cutting system of the longwall shearers. In the article, the speed control of the induction motors is built on sensorless vector control systems, with direct orientation after the rotor fluxes (see CS_1, CS_2, CS_R and CS_R in the previous figures).

Within these control systems, the estimation of the position and dq components of the rotor flux space-phasor, as well as the rotor speed of the induction motor, are done by an

extended Gopinath observer (EGO) [5]. The control systems of induction motor speeds in the mining machines are of the same type. The block diagram of a speed control system for induction motors is presented in Fig. 10.

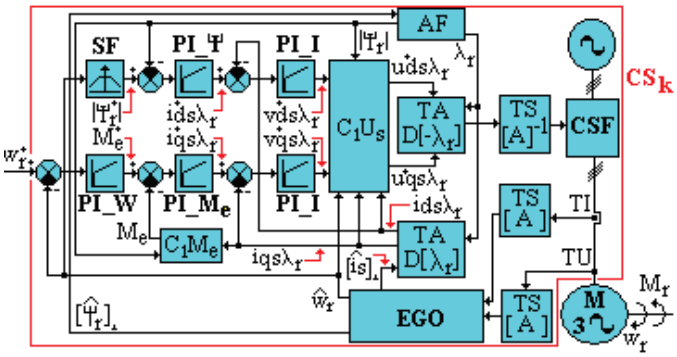

Fig.10. The sensorless vector control system of the speed induction motor.

In the following, we will present the mathematical equations that define the main blocks of the control system [3], [5], presented in Fig. 10.

- *The analyzer block of the rotor flux phasor* (*AF*). The equations defining the phasor module and position of the rotor flux are:

$$\psi_r = \left|\underline{\psi}_r\right| = \sqrt{\psi_{dr}^2 + \psi_{qr}^2} \tag{17}$$

$$\sin\lambda_r = \frac{\psi_{qr}}{\psi_r}; \quad \cos\lambda_r = \frac{\psi_{dr}}{\psi_r} \tag{18}$$

- *Extended Gopinath Observer (EGO)*. The equations that define this type the observer are presented on the following relations [5]

$$\frac{d}{dt}x = A_a \cdot x + A_b \cdot x + B \cdot u + \underline{G} \cdot C \cdot \frac{d}{dt}e_x \tag{19}$$

$$\hat{\omega}_r(t) = k_R \cdot \varepsilon(t) + \frac{k_R}{T_R} \cdot \int_0^t \varepsilon(\tau) \cdot d\tau \tag{20}$$

where $x = \left[\underline{i}_s \quad \underline{\psi}_r\right]^T$; $x = \left[\underline{\hat{i}}_s \quad \underline{\psi}_r\right]^T$; $e_x = x - x$;

$$A_a = \begin{bmatrix} a_a^* & a_{12}^* \\ 0 & a_{22}^* \end{bmatrix}; A_b = \begin{bmatrix} a_b^* & 0 \\ a_{21}^* & 0 \end{bmatrix}; B = \begin{bmatrix} b_{11}^* \\ 0 \end{bmatrix}; \underline{G} = \begin{bmatrix} 0 \\ \underline{g} \end{bmatrix}; C = [1 \quad 0];$$

$$a_{11}^* = a_a^* + a_b^*; a_{21}^* = a_{31}^*; a_{31}^* = \frac{L_m^*}{T_r^*}; a_{12}^* = a_{13}^* - j \cdot a_{14}^* \cdot z_p \cdot \omega_r;$$

$$a_{22}^* = a_{33}^* + j \cdot z_p \cdot \omega_r; \; a_{33}^* = \frac{-1}{T_r^*}; \; b_{11}^* = \frac{1}{L_s^* \cdot \sigma^*};$$

$$a_{13}^* = \frac{L_m^*}{L_s^* \cdot L_r^* \cdot T_r^* \cdot \sigma^*}; a_{14}^* = \frac{L_m^*}{L_s^* \cdot L_r^* \cdot \sigma^*}; T_s^* = \frac{L_s^*}{R_s^*}; \; T_r^* = \frac{L_r^*}{R_r^*};$$

$$\sigma^* = 1 - \frac{\left(L_m^*\right)^2}{L_s^* \cdot L_r^*}; \; a_a^* = -\frac{1}{T_s^* \cdot \sigma^*}; \; a_b^* = -\frac{1 - \sigma^*}{T_r^* \cdot \sigma^*};$$

$$\varepsilon = e_1 \cdot \psi_{qr} - e_2 \cdot \psi_{dr}; \; e_1 = i_{ds} - \hat{i}_{ds}; \; e_2 = i_{qs} - \hat{i}_{qs};$$

$$u = \underline{u}_s; \; \underline{i}_s = i_{ds} + j \cdot i_{qs}; \; \underline{\psi}_r = \psi_{dr} + j \cdot \psi_{qr}; \; \underline{u}_s = u_{ds} + j \cdot u_{qs};$$

$$\underline{\hat{i}}_s = \hat{i}_{ds} + j \cdot \hat{i}_{qs}; \; \underline{\hat{\psi}}_r = \hat{\psi}_{dr} + j \cdot \hat{\psi}_{qr}; \; \underline{g} = g_a + j \cdot g_b.$$

The coefficients which define the Gopinath matrix G, are [5]:

$$g_a = -k \cdot \frac{a_{31}^* \cdot a_{33}^*}{\left(a_{33}^*\right)^2 + \left(z_p \cdot \omega_r\right)^2} \tag{21}$$

$$g_b = k \cdot \frac{a_{31}^* \cdot z_p \cdot \omega_r}{\left(a_{33}^*\right)^2 + \left(z_p \cdot \omega_r\right)^2} \tag{22}$$

where k is a coefficient of proportionality ($k > 0$).

In the above relations, we marked with „*”, the electrical parameters, determined experimentally, of the induction motor.

The dynamic controlling of the speed observer is done via constants k_R and T_R. The other blocks of Fig.10, are presented in detail in [5], [6].

VI. The Coal Flow Control System

The constant control of the flow of coal on the scraper conveyor currently accounts for one of the most important issues in the field of automation of longwall systems.

The most significant consumption of electricity in coal exploitation in mining of coal is due to electric motors in the transmission of coal flow in an underground silo, and then, with the help of the extraction machine, at the surface.

The electric motors from the conveyor flux component are oversized, which entail a very high consumption of electric energy.

The advantage of a system to control the flow of coal on the scraper conveyor is that electric motors from the flow of transport can be optimal chosen, leading ultimately to a much lower consumption of electricity for coal extraction.

In order to design the control system of the flow of coal on the scraper conveyor, in the following we will define the masic flow rate cut by the longwall shearer. It is given by the following relation:

$$Q_c = \rho_a \cdot v_a \cdot A_a \cdot \delta(v_t) \tag{23}$$

where Q_c is the masic flow of coal that is achieved by the longwall shearer, $A_a = B \cdot H$ the domain of the area exploited, B is the width cute of the longwall shearer, H is the height cute of the longwall shearer, ρ_a is the average density of coal, and v_a is the advance speed of the longwall shearer, δ is Kronecker function.

The flow of loading coal on the scraper conveyor using two cutting devices is given by the following relation [7]:

$$Q_i = k_c \cdot \rho_a \cdot v_t \cdot A_b \tag{24}$$

where Q_i is the mass of coal loaded on the scraper conveyor, $A_b = \pi \cdot \left(R_a^2 - R_b^2\right)$ is the area of the snail section; R_a is the radius of the cutting; R_b is the radius of the hub cutting organs; v_t is the cutting speed; ρ_a is the average density of coal; k_c is a dimensionless coefficient.

Under these conditions, in the dynamical regime can write the following differential equation:

$$Q_c(t) - Q_i(t) = \frac{dM(t)}{dt} \tag{25}$$

where M is the mass of accumulated coal on the hearth between the conveyor and the coal massive.

In the context of the relationship (25) is observed that, in order to reduce the mass of coal left on the hearth, the mass flow rates must satisfy the following equality $Q_c \cong Q_i$.

Under these conditions, the equality $Q_c \cong Q_i$, can be put under the following form

$$v_t \cong \frac{A_a}{k_c \cdot A_b} \cdot v_a \tag{26}$$

The relation (26) has an essential role in the proposed control system. From relation (26) and (7), obtain:

$$\frac{k_b \cdot \tan(\psi)}{2 \cdot d - b} \cong \frac{A_a}{k_c \cdot A_b} \tag{27}$$

If the relationship (27) is respected, remaining coal mass variation is very small.

In these conditions, the load per unit length of the scraper conveyor is given by the following relations:

$$q = \frac{Q_c}{v_t} = \rho_a \cdot A_a \cdot \frac{v_a}{v_t} \cdot \delta(v_t) \tag{28}$$

In the context of the relation (28), coal load per unit length of the scraper conveyor can be controlled on the basis of the ratio of the advancement speed and the cutting speed, respecting the condition (7) and (27).

In order to control the mass flow of coal on the scraper conveyor, in the following we will keep in mind that the masic flow rate of the conveyor is given by the following relation

$$Q_{tr} = q \cdot v_{tr} \tag{29}$$

where q is the loads of charcoal per unit length of the conveyor and v_{tr} is the speed of the conveyor.

In the relation (29) is observed that when the speed v_{tr}, is maintained constant, mass flow control of coal on the scraper conveyor can be done by modifying the cargo of coal per unit length of the conveyer. In other words, the mass flow rate control of the conveyor is provided by means of the ratio between the advance speed and the cutting speed.

The mass flow measurement of coal that is at some point of time on the conveyor is provided by means of a scale with continuous measurement (FT).

On the other hand, is observed that when the conveyor speed is chosen based on the following relation:

$$v_{tr}^* = \frac{v_t^*}{2} \tag{30}$$

the mass flow of coal from the conveyor is:

$$Q_{tr} = \rho_a \cdot A_a \cdot \frac{v_a}{2} \cdot \delta(v_t) \tag{31}$$

The relation (31) reveals that the mass flow of coal from the conveyor can be controlled directly through the advancement speed, if the expression (30) is satisfied.

The speed control system of the conveyor is presented in Fig.11 [3].

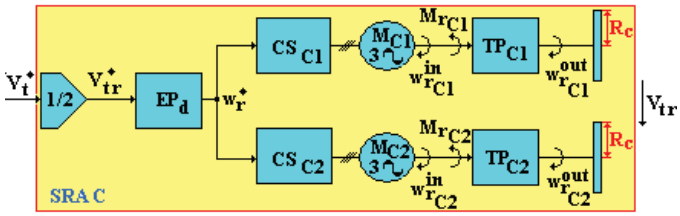

Fig.11. The block diagram of the speed control system of the conveyor.

The system consists of two conveyors (T_1 and T_2), electrically operated through two induction motors (M_{C1} and M_{C2}).

The speed of the two induction motors is controlled via two sensorless vector control systems (CS_{C1} and CS_{C2}).

The control systems for the speed of the induction motors in the scraper conveyors component have the same form as in Fig.10.

The electromagnetic torques and the speeds of the two induction motors are submitted to the drive mechanisms of the conveyors, using the planetary transmissions (TP_{C1} and TP_{C2}).

On the other hand, the prescribing element (EP_d) of the speed of the two control systems is defined by the following relation

$$\omega_r^* = \frac{i_{tr}}{R_c} \cdot v_{tr}^* \tag{32}$$

where i_{tr} is the gear transmission ratio for TP_{C1} and TP_{C2}, and R_c is the reel radius by drive.

The equation that define the planetary transmissions (TP_{C1} and TP_{C2}), is identical with (32).

The block diagram of the control system of the mass flow of coal, of the scraper conveyor, based on equation (31), is shown in Fig. 12.

The automatic controller of the mass flow (PI_F), is one of the integral proportional type.

The weighing scale is placed on the scraper conveyor, located outside the hewing coal.

Due to the above considerations, the mathematical model is affected by a dead time.

The dead time can be calculated as in the following relation:

$$T_m = \frac{L_c(t)}{v_{tr}} \tag{33}$$

where $L_c(t) = L_a(t) + L_b$ is distance (the position) of the longwall shearer compared with the measurement element to the flow mass (the weighing scale conveyor).

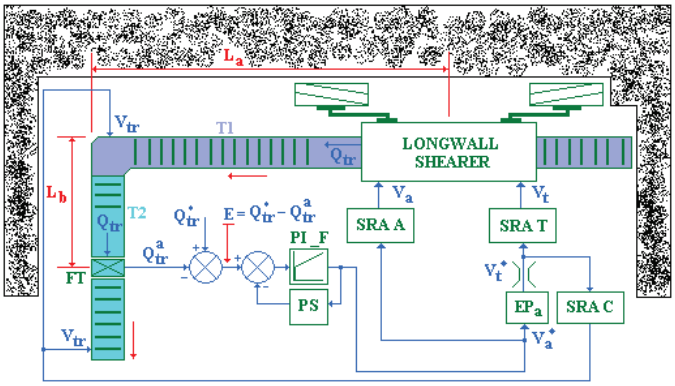

Fig.12. The coal flow control system of on the scraper conveyor [3].

The coal flow Q_{tr}^a (see Fig.12), is affected by a dead time. The mathematical equation that define this flow of coal, is:

$$Q_{tr}^a(s) = Q_{tr}(s) \cdot e^{-T_m \cdot s} \tag{34}$$

where $T_m = L_c / v_{tr}$; $L_c = L_a + L_b$; L_b is a constant distance and the L_a is a variable distance.

In the relation (34), variable $s \in C$ it results from applying Laplace transform. To compensate for dead time effects, we use the control strategy that uses a Smith predictor (SP) [8].

VII. Analysis By Simulation Of The Control System

The simulation of the control system proposed is based on the equations presented in the article and the block diagram in Fig. 12. The simulation is performed in Matlab-Simulink [9], [10]. In the simulation of the control systems at the advancement and cutting speeds of the longwall shearer, are taken into account the dynamic effects introduced by static frequency converter (CSF). Switching frequency of the IGBT transistors in the inverter is 2 kHz. The equations that define the resistance torques are presented in detail in [3].

The electrical and mechanical parameters of the induction motor from the control system component of the flow of the coal are presented below:

- the electrical and mechanical parameters of the induction motors from the advancement system:

$$P_n = 45[\text{kW}];\ U_n = 440[\text{V}];\ I_n = 74[\text{A}];\ z_p = 2;$$
$$n_n = 1459[\text{rot/min}];\ M_n = 295[\text{N}\cdot\text{m}];\ L_s = L_r = 0.0253[\text{H}];$$
$$L_m = 0.024823[\text{H}];\ R_s = 0.229133[\Omega];\ R_r = 0.096662[\Omega];$$
$$J = 0.17[\text{kg}\cdot\text{m}^2];\ F = 0.028[\text{N}\cdot\text{m}\cdot\text{s/rad}];\ \eta_n = 90[\%];$$
$$f_n = 50[\text{Hz}];\ \cos(\varphi) = 0.98$$

- the electrical and mechanical parameters of the induction motors from the cutting system:

$$P_n = 200[\text{kW}];\ U_n = 1000[\text{V}];\ I_n = 155[\text{A}];\ z_p = 2;$$
$$n_n = 1470[\text{rot/min}];\ M_n = 1300[\text{N}\cdot\text{m}];\ L_s = L_r = 0.0224[\text{H}];$$
$$L_m = 0.021507[\text{H}];\ R_s = 0.137388[\Omega];\ R_r = 0.083842[\Omega];$$
$$J = 2.2[\text{kg}\cdot\text{m}^2];\ F = 0.06[\text{N}\cdot\text{m}\cdot\text{s/rad}];\ \eta_n = 93.5[\%];$$
$$f_n = 50[\text{Hz}];\ \cos(\varphi) = 0.8$$

- the electrical and mechanical parameters of the induction motors from the scraper conveyors:

$$P_n = 200[\text{kW}];\ U_n = 1000[\text{V}];\ I_n = 142[\text{A}];\ z_p = 2;$$
$$n_n = 1480[\text{rot/min}];\ M_n = 1290[\text{N}\cdot\text{m}];\ L_s = L_r = 0.0273[\text{H}];$$
$$L_m = 0.026736[\text{H}];\ R_s = 0.14769[\Omega];\ R_r = 0.058708[\Omega];$$
$$J = 5.8[\text{kg}\cdot\text{m}^2];\ F = 0.065[\text{N}\cdot\text{m}\cdot\text{s/rad}];\ \eta_n = 94.5[\%];$$
$$f_n = 50[\text{Hz}];\ \cos(\varphi) = 0.86$$

The mechanical parameters of the gears and the main technical data of the longwall shearer and scraper conveyor are given below:

- The gear ratios of the gear units: $i_A = 196.185$; $i_T = 36.725$; $i_{tr} = 33$.
- The radius of the wheels drive: $R_a = 0.6[\text{m}]$; $R = 0.179[\text{m}]$; $R_c = 0.23[\text{m}]$; $R_b = 0.225[\text{m}]$.
- The other parameters used in the simulation are:

$$c = 2;\ d = 0.05[\text{m}];\ b = 0.015[\text{m}];\ H = 2[\text{m}];$$
$$B = 0.6[\text{m}];\ \tan(\psi) = 1.28;\ L_b = 5[\text{m}].$$

For the tuning of PI controllers from the control system component in Fig.2, we used the following values of the constants T_{d1}^* and T_{d2}^*:

- For SRA T and SRA C: $T_{d1}^* = 3 \cdot 10^{-3}$; $T_{d2}^* = 6 \cdot 10^{-3}$
- For SRA A: $T_{d1}^* = 3 \cdot 10^{-3}$; $T_{d2}^* = 9 \cdot 10^{-3}$

Parameters that define the extended Gopinath observer are:

$$k = 0.2;\ k_R = \frac{1}{T_{d1}^* \cdot k_u};\ T_R = \frac{T_r^*}{2}$$

where: $k_u = a_{14} \cdot z_p \cdot \psi_r^*$; $\psi_r^* = \frac{U_{\max}}{2 \cdot \pi \cdot f_N}$; $U_{\max} = U_n \cdot \frac{\sqrt{2}}{\sqrt{3}}$.

This dead time in the process of the model makes it difficult the control the flow of coal by the scraper conveyor.

In this sense, the parameters which defining the PI (Proportional Integral) flow control are:

$$k_q = \frac{T_{d1}^*}{30};\ T_q = \frac{10}{3} \cdot T_{d1}^*$$

To compensate for dead time effects, we use the control strategy that uses a Smith predictor [8]. So, the transfer function of the Smith predictor used is:

$$G_H(s) = G_0(s) \cdot \left(1 - e^{-T_m \cdot s}\right) \quad (35)$$

where $G_0(s) = \dfrac{a_1 \cdot s + a_0}{s^2 + b_1 \cdot s + b_0}$, and the coefficients that define the transfer function are: $b_1 = 52$; $b_0 = 65^2$; $a_1 = -479.4521$; $a_0 = 2.026 \cdot 10^6$.

In these conditions, the simulation program and the simulation results are presented in the following.

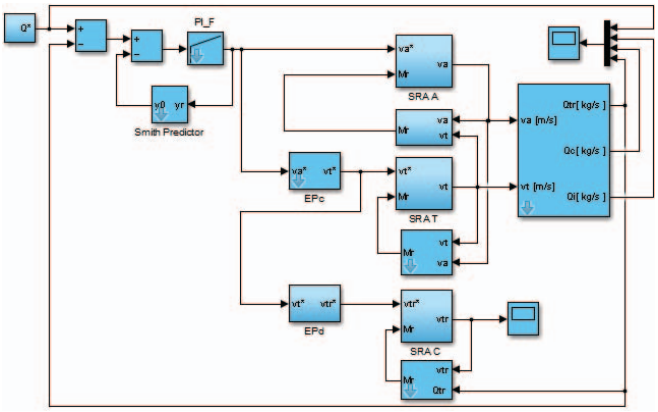

Fig.13. The simulation program of the coal flow control system.

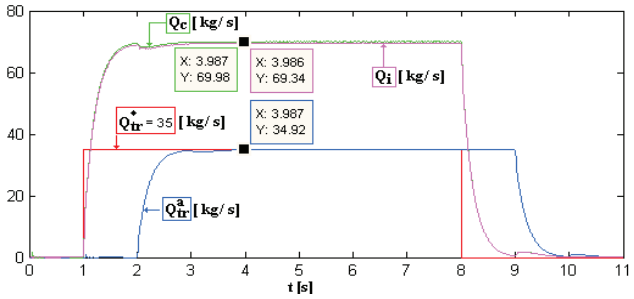

Fig.14. The step response of the coal flow control system – case 1.

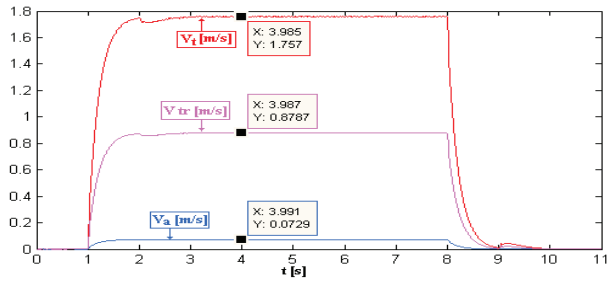

Fig.15. The time variation of the speeds (v_a, v_t and v_{tr}) – case 1.

From the graphs of Figures 14 and 15, it is observed that when coal flow imposed is 35 [kg/s], advance speed is stabilized at 4.374 [m/min].

The cutting speed is stabilized at 1.75 [m/s] and conveyor speed is 0.87 [m/s].

From the graphs of Figures 16 and 17, it is observed that when coal flow imposed is 20 [kg/s], advancement speed stabilizes at 2.499 [m/min]. In this case, the cutting speed is stabilized to 1 [m/s] and conveyor speed is by 0.5 [m/s].

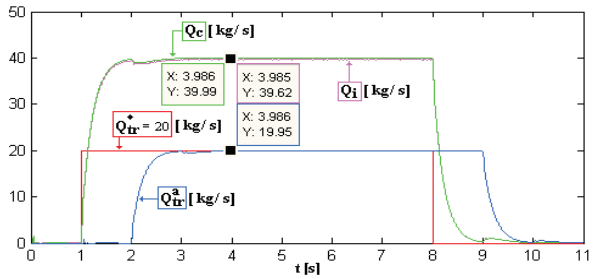

Fig.16. The step response of the coal flow control system – case 2.

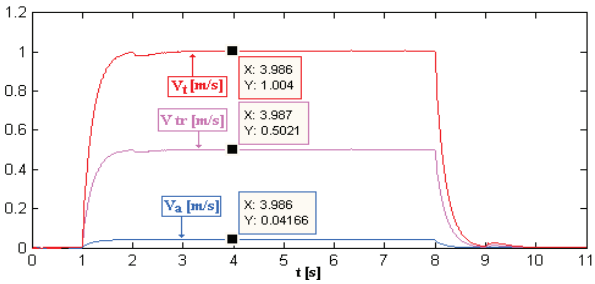

Fig.17. The time variation of the speeds (v_a, v_t and v_{tr}) – case 2.

VIII. CONCLUSIONS

In this article, the modeling and simulation of a new coal flow control system for the longwall scraper conveyor is presented.

After analyzing by simulation in the Matlab-Simulink of the coal flow control system, we find that the control system works properly, having good dynamic performances. Given the above, we believe that the control system of the coal flow, presented in this article, can be successfully used in practice.

Received on July 20, 2016
Editorial Approval on November 15, 2016

REFERENCES

[1] I. Kovacs, N. Ilias, M.S. Nan, "The Working Regime of the Cutter Loaders", Universitas Publishing House, Petrosani, 2000.

[2] ***, www.cat.com

[3] O. Stoicuta, T. Pana, C. Mandrescu, "The Control System Analisys of the Coal Flow on the Scrapers Conveyor in a Longwall Mining System", Int. Conf. IEEE ICATE, Oct. 2016.

[4] ***, The technical documentation of the longwall shearer - KSW460NE, www.kopex.com.pl

[5] Pana T., Stoicuta O., "Small Speed Asymptotic Stability Study of an Induction Motor Sensorless Speed Control System with Extended Gopinath Observer", Journal of Advances in Electrical and Computer Engineering, vol.11, no.2, pp.15-22, 2011.

[6] T.Pana, O. Stoicuta, "Controllers Tuning for the Speed Vector Control of Induction Motor Drive Systems", Int. Conf. IEEE AQTR, vol.1, pp.1-6, May 2010.

[7] S.S.Peng, H.S. Chiang, Longwall Mining, John Wiley&Sons, 1984.

[8] O.J. Smith, "A Controller to Overcome Dead Time", ISA J., vol.6, no.2, pp. 28-33, Feb. 1959.

[9] C.H. Ong, "Dynamic Simulations of Electric Machinery: using Matlab/Simulink", Prentice Hall, 1998.

[10] T. Pană, "Matlab Application Toolbox – Electrical Drives – Induction Motor", Mediamira Publishers, Cluj-Napoca, Romania, 1997.